Front. Struct. Civ. Eng. 2018, 12(3): 331–340
https://doi.org/10.1007/s11709-017-0421-y

RESEARCH ARTICLE

Damage on lining concrete in highway tunnels under combined sulfate and chloride attack

Rongrong YIN*, Chenchen ZHANG, Qing WU, Baocheng LI, He XIE

School of Architeture and Civil Engineering, Jiangsu University of Science and Technology, Zhenjiang 212003, China
**Corresponding author. E-mail: ecsi_tangjian@163.com*

ABSTRACT The combined effect from sulfate and chloride is one of the important reasons to cause the damage of lining concrete in highway tunnels. To investigate the effect of chloride ions on the corrosion of lining concretes under sulfate attack, ultrasonic detecting, compression test and X-ray Diffraction (XRD) were performed on the concretes to obtain the ultrasonic velocity, corrosion thickness, compression strength and corrosion products. The ultrasonic results, compression strength and XRD patterns confirmed that the existence of chloride certainly depressed the corrosion damage on the lining concretes under sulfate attack, and the depressing effect increased with the content of chloride in the composite solution. The corrosion damage on the concretes experienced three stages independent of the composition of corrosive solution: initial slower enhancement on the strength, stabilization period and linear degradation period. The existence of chloride mainly affected the final degradation stage and obviously decreased the corrosion thickness.

KEYWORDS lining concrete, sulfate, chloride, compression, ultrasonic

1 Introduction

In recent years, damage is always occurred in the lining concretes for highway tunnels. There are many factors to cause this problem, and one of the most important reasons is the corrosion on the lining structure caused by the corrosive environmental water, which has been world widely reported such as in Italy [1,2], European area [3–5], Japan [6,7], etc. Usually, corrosive substances in the environmental water have combined effects on the lining structure, mainly from the interaction of sulfate and chloride. For example, in eastern China, large amounts of chloride and sulfate ions are existed in the sea water, and correspondingly the coupled erosions of chloride and sulfate ions on the damage of concrete must be considered during the construction of river or sea crossed tunnels near the marine environment [8,9]. Similarly, in southwest China and western Salt Lake area, not only the single sulfate solution but also the high content sodium chloride solution is attributed to the corrosion of lining concrete [10].

Previous studies on the damage of concrete were mainly based on the erosion of single corrosive medium. Chen et al. [11] studied the damage evolution of cement mortar under the solution of sodium sulfate and concluded that the average size of microvoids in cement mortar affected the damage evolution significantly Chu and Chen [12] introduced a simple ultrasonic technique to evaluate the damage evolution in concrete under sulfate attack and built a relationship between the magnitude of the attenuation coefficient of concrete, the wave velocity of the elastic dilation wave and the damage evolution. However, the damage evolution process is seldom studied under combined effect from sulfate and chloride. And the understanding of the interaction mechanism between the two salts is highly debated and inconclusive. Brown et al. [13] drew a conclusion that Friedel's salt was formed among sulfate corrosion products due to the existence of chloride. Al-Amoudi et al. [14] observed the corrosion phenomena under combined environments for different kinds of concrete. Results indicated that the presence of chloride ions in the sulfate environments mitigated the sulfate attack in plain and blended cements. The performance of blended cements was observed to depend on the type of mineral admixture used, both in the sulfate and the sulfate-chloride environments. Tumidajski et al.

Article history: Received Nov 1, 2016; Accepted Feb 23, 2017

[15] found that sulfate and CO_2 decreased the chloride penetration and diffusivity in ordinary Portland cement concrete. Jin [16] studied the effect of concrete composition and chloride on damage of concrete attacked by sulfate, and found that the damage resistance of concrete was improved by the chloride in sulfate solution and also by the lower water-to-binder ratio or suitable addition of fly ash in the concrete. Reju et al. [17] investigated the chemical attack related durability properties of ultra high performance fibre reinforced concrete (UHPFEC) under acids, sulfate and chlorides. Results indicated that UHPFRC was resistance to attack of acids, while corrosion resistance properties became worse in sulfates and chlorides. Al-Amoudi et al. [18] studied the reinforcement corrosion phenomena in marine environments and in soils contaminated with high concentrations of chloride and sulfate salts. The longer time to initiation of corrosion was observed in single sulfates. Corrosion current density increased a lot when the concentration of chloride and sulfate salts was beyond the threshold level. Change on strength of self-consolidating concretes and ordinary concretes with different W/C ratio under sodium sulfate and sodium sulfate/sodium chloride combined solutions, and concluded that the influence of chloride on increasing sulfate attack was more significant for high W/C concretes [19]. Pradhan [20] studied the corrosion behavior of steel reinforcement in concrete under the composite chloride-sulfate solution. On the corrosion behavior of lining concrete in highway tunnels, Chen [21] studied the cracked concrete permeability under chloride attack, water pressure and crack width. Pan et al. [22] built a model of carbonation depth of underground concrete structure including the effect of stress, W/C ratio and operation periods. Lei [23] studied the mechanical properties of lining concrete in tunnel structure under sulfate attack.

Therefore, there was little works on the combined attack from chloride and sulfate on the concretes. In this paper, through simulating the transport of corrosive ions in the solution, the effect of existence of chloride in sulfate solution on the corrosion in lining concretes was studied. Corrosive damage on the concrete is usually evaluated with the corrosion thickness or compressive strength, and the corrosion thickness can be measured using ultrasonic detection on prismatic concretes or strength degradation method on cubic concretes [24]. In this paper, the influence of chloride on the corrosion of lining concrete in highway tunnels under sulfate attack was studied through simulating the transport of corrosive solution into concrete. Sulfate solution, chloride solution and composite sulfate-chloride solution were used as the corrosive solution, respectively. Ultrasonic penetration testing on prismatic concrete samples was introduced to measure the corrosion thickness through the sound velocity. Combined with the compression strength, the effect of chloride on lining concrete was studied under the sulfate attack, and was finally verified with X-ray diffraction (XRD).

2 Experimental

2.1 Specimens

A 425# ordinary Portland cement, which suggests the strength of concrete will be greater than 42.5 MPa after curing with water for 28 days, is chosen as specimen material with the composition contained 22.5wt% SiO_2, 52.7wt% CaO, 3.95wt% MgO, 13.01wt% Al_2O_3, 2.63wt% SO_3, and 2.91wt% Fe_2O_3. Prismatic concrete specimens of 100 mm × 100 mm × 300 mm were cast using cement, water, fine aggregates and coarse aggregates with the mixing ratio of 1:0.41:1.33:2.65. The size of the coarse aggregates was kept to less than 25 mm. After the water curing period of 28 days, the cube concrete was mechanical tested with the compression strength of 33.45 MPa.

2.2 Corrosion tests

Four types of solution were prepared for the erosion experiment with the composition listed in Table 1. Group A is the water for the comparison. The others are 10% sodium sulfate solution (Group B), 10% sodium sulfate + 5% sodium chloride composite solution (Group C) and 10% sodium sulfate + 10% sodium chloride composite solution (Group D), respectively. To simulate the corrosion on lining concrete in tunnels, four sides of each prismatic concrete were paraffin-sealed, and then the specimens with total numbers of 96 were immersed into the above solutions with the immersed depth of 150 mm. Three specimens were taken out from each solution every 30 days.

Table 1 Details on corrosion test

Group	Concentration (%)		Number of specimens
	Na_2SO_4	NaCl	
A	0	0	24
B	10	0	24
C	10	5	24
D	10	10	24

2.3 Experimental methods

Ultrasonic tests were conducted on the specimens with ZBL-U5200 ultrasonic detector. The diameter of detector was 30 mm, the frequency was 50 kHz and the couplant was vaseline. Fig. 1 shows the details on opposite testing method. Five locations in each concrete were tested to obtain the average on the time of ultrasonic propagation (t). The ultrasonic sound velocity V was then calculated by Eq. (1):

$$V = l/t, \tag{1}$$

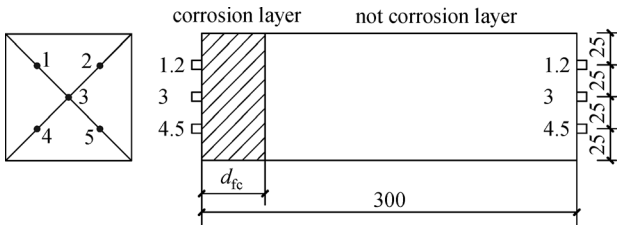

Fig. 1 Sketch on opposite measure method for ultrasonic testing

where l is the distance on ultrasonic propagation and equals to the height of specimen (300 mm).

The compression test was finished on YAW-2000 compression tester with the loading rate of 2 kN/s.

To identify the phases formed in the lining concretes during corrosion, the cement paste was prepared for X-ray Diffraction (XRD, LabX XRD-6000). The microstructure was also observed by JEOL JSM6480 scanning electron microscopy (SEM).

3 Results and discussion

3.1 Ultrasonic velocity

Three prismatic concretes without immersion were randomly selected to measure the initial ultrasonic time. The average time is 61.573 μs. The samples in the water and different corrosive solution for 0–240 days were also detected with ultrasonic, and the results are shown in Fig. 2(a). Through the Eq. (1), the ultrasonic sound velocity was calculated, as shown in Fig. 2(b). It can also be found there were no obvious differences on the initial ultrasonic times for the concretes without corrosion in each group, which suggested that the casted concretes were satisfied with the stand quality. After the concretes were immersed into the water, the ultrasonic sound velocity was gradually increased with the immersion time due to the curing effect from clean water. After the concretes were immersed into the corrosive solutions, the velocity firstly increased with the corrosion time until 90 days because the nucleation and growth of ettringite in specimens, by which the density of concretes was increased to accelerate the propagation on ultrasonic wave. After that, the velocity decreased with the corrosion time. Compared the chloride-contained sulfate solution with 10% sulfate solution, the existence of chloride in the corrosive solution obviously depressed the decrease on the ultrasonic velocity. Therefore, the corrosion on the lining concretes was still occurred in the chloride-sulfate composite solution, but the addition of chloride effectively depressed its corrosion under sulfate attack.

3.2 Compression strength

Fig. 3 shows the results of compressive strength on lining concrete samples with the effect of corrosive solution and immersion time. For samples in the water (Group A), the compressive strength increased with exposure time up to 90 days, and then kept stable from 90 to 240 days. For samples in the sulfate solution (Group B), the compressive strength initially increased with time from 0 to 90 days, but rapidly decreased due to obvious corrosion from sulfate ions attack on the concretes. For samples in the composite solution (Group C and D), the change on the compressive strength with immersion time was similar as that in the water, i.e. initially increased with the time and then kept stable after 90 days, which is possibly attributed to the reason that the density of concretes increased from the crystallization in the concretes. It also should be noted that there existed a smaller effect on the compressive strength from the corrosion thickness for prismatic concretes compared with cubic concretes, and then the change on the strength was not obviously observed in this paper [25].

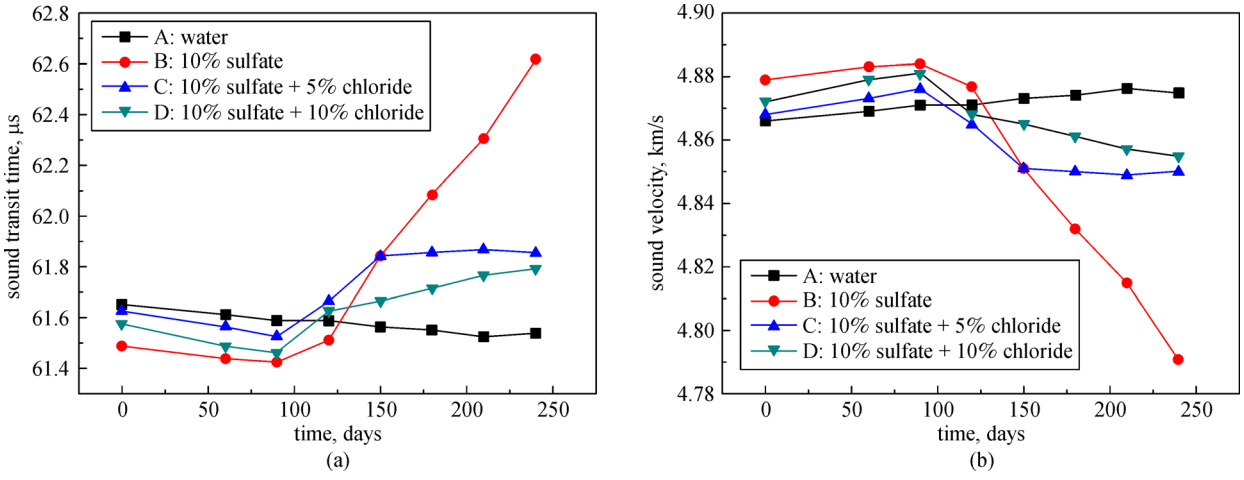

Fig. 2 Relationship between immersion time and ultrasonic transit time (a) and velocity (b) in the lining concretes with different corrosive solution

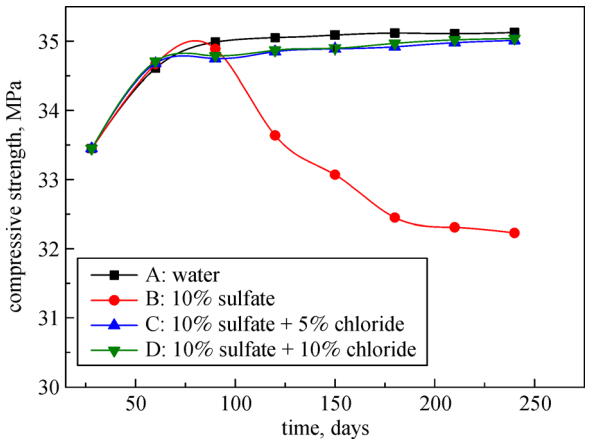

Fig. 3 Relationship between the compressive strength on the lining concretes and immersion time considering the effect of change on the corrosive solution

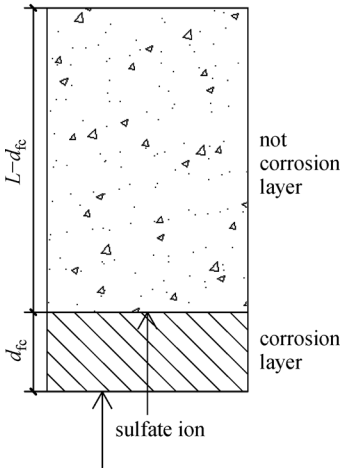

Fig. 4 Corrosion layer division of specimen

3.3 Corrosion thickness

Fig. 4 shows a simple diffusion model including the corrosion thickness on the concrete under sulfate attack. The specimen was proposed to be a homogeneous and continuous material. The relationship between ultrasonic velocity and corrosion thickness can be expressed by Eq. (2) [25]:

$$\frac{S_s}{S_0} = \frac{(L-d_s)\frac{L}{3}}{\frac{L^2}{3}} = \frac{V_s^2}{V_0^2}, \tag{2}$$

where S_0 is cross-sectional area before damage, and can be calculated with Eq. (3):

$$S_0 = \frac{L^2}{3}, \tag{3}$$

where L is the length of specimen and equals to 300 mm, and d_s is the corrosion thickness.

S_S is the cross-sectional area after damage, and is calculated with Eq. (4):

$$S_s = (L-d_s)\frac{L}{3}. \tag{4}$$

V_S is the ultrasonic velocity on the damaged concrete with the existence of corrosion thickness, and is calculated by Eq. (5):

$$V_s = \frac{L}{T_s}, \tag{5}$$

where T_S is the ultrasonic transit time on the damaged concrete.

V_0 is the ultrasonic velocity on the initial concrete without corrosion, and is calculated by Eq. (6):

$$V_0 = \frac{L}{T_0}, \tag{6}$$

where T_0 is the ultrasonic transit time on the undamaged concrete.

And the corrosion thickness can be calculated with Eq. (7):

$$d_{fc} = d_S = \frac{(V_0^2 - V_s^2)L}{V_0^2}. \tag{7}$$

During ultrasonic testing, the emission and receiving transducers should be in a parallel line, the transmitting time across the concrete was recorded and the corrosion thickness was calculated using the method of $V_S - V_0$ with the results shown in Table 2. The relationship between corrosion thickness and immersion time in different corrosive solutions and water was then plotted in Fig. 5.

For samples in the water in Group A, the corrosion thickness of lining concretes always kept the negative

Table 2 Corrosion thickness on the specimen in four groups

Group	Corrosion thickness (mm)							
	0 d	60 d	90 d	120 d	150 d	180 d	210 d	240 d
A	0	−0.376	−0.627	−0.878	−1.255	−2.009	−1.883	−2.135
B	0	−0.729	−1.094	1.698	3.875	6.284	9.879	12.858
C	0	−0.740	−0.987	0.370	2.092	2.214	2.337	2.214
D	0	−0.728	−0.971	0.364	1.090	1.453	1.574	1.937

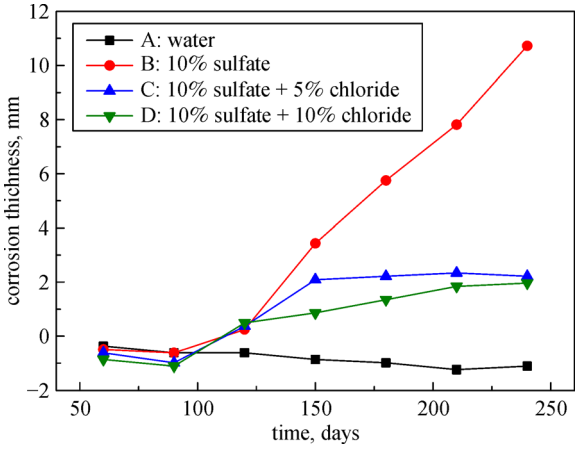

Fig. 5 Relationship between the corrosion thickness and immersion time

value and slowly increased with the immersion time, because the density of concretes increased with the time due to the curing effect from water, and correspondingly it took a shorter time for the propagation of ultrasonic wave in the samples. For samples in Na_2SO_4 solution in Group B, the corrosion thickness of concrete was negative value with a certain degree of negative growth before 90 days because of the enrichment of corrosion products in the concrete during the earlier stage. After 90 days, the corrosion thickness became positive and linearly increased with the corrosion time. For samples in NaCl-Na_2SO_4 composite solution in Group C or D, the change on the corrosion thickness during the earlier immersion time was similar as the trend in solution A or B. However, the corrosion thickness slowly increased with the immersion time after 90 days with the growing rate far slower than that in Na_2SO_4 solution. Compared the results in solution C and D with the effect of content of NaCl in Na_2SO_4 solution, the corrosion thickness in 10% sodium sulfate + 10% sodium chloride composite solution (Group D) rapidly increased to about 2 mm with the time from 90 to 150 days, and then kept constant after 150 days, but the corrosion thickness in 10% sodium sulfate + 5% sodium chloride composite solution (Group C) gradually increased with immersion time from 90 to 240 days, and finally reached the similar thickness as in Group D. Therefore, the existence of chloride in the composite solution was beneficial to depress the growth on corrosion thickness, and the depressing effect increased with the content of chloride in the solution.

From Fig. 5, there existed three stages on the compression strength of concretes on the immersion time-corrosion thickness curves independent of the kind of corrosive solutions: initial slower enhancement on the strength, stabilization period and linear degradation period. The addition of chloride into the corrosive solution mainly affected the linear degradation period, and obviously depressed the growth of corrosion thickness with immersion time. In a lower content of chloride in the composite solution, a prolonged degradation period was required for the corrosion of concrete. However, with the increase on the content of chloride in the composite solution, the corrosion thickness quickly reached the maximum, and then kept constant.

In the combined chloride-sulfate solution, due to the faster diffusion rate of Cl^- than that of SO_4^{2-}, the chemical replacement reaction between Cl^- from the corrosive solution and OH^- from the concretes was firstly occurred to decrease on the PH value of the concrete, which promotes the dissolution of ettringite (AFt) formed from the sulfate attack. On the other hand, Cl^- was also reacted with the hydrated calcium aluminate ($3CaO \cdot Al_2O_3 \cdot 6H_2O$) in concretes to produce $3CaO \cdot Al_2O_3 \cdot 3CaCl_2 \cdot 3H_2O$ Friedel salts. The decrease on the amounts of ettringite crystals reduced the corrosive attack from sulfate, and the depressing effect was increased with the content of Cl^- in the solution.

3.4 Compositions on corrosion products

Fig. 6 shows the XRD spectrums on the cement pastes from the concrete specimens immersed into A solution (water, Figs. 6(a) and 6(b)), B solution (10% Na_2SO_4 solution, Figs. 6(c) and 6(d)) and D solution (10% NaCl + 10% Na_2SO_4 composite solution, Figs. 6(e) and 6(f)) for 60 days and 120 days, respectively.

The integrated intensity of the diffraction peak is directly proportional to the total number of involved diffraction planes, while the number of involved diffraction planes depends on the total volume of its crystalline state which is in the range of the X-ray beam [26,27]. Compared Figs. 6(a) and 6(b) for the specimens in the water, the only difference is the intensity of Calcium Silicate Hydrate (CSH) because the prolonged immersion time in the water was beneficial the reaction between water and cement to produce more CSH in the concrete. Compared the results in Figs. 6(e) and 6(f) with Figs. 6(c) and 6(d), the intensity and half-height width of peak at the 2θ of 43 degree reflecting calcium hydroxide (CH) phase was stronger and wider for the samples immersed in solution D due to the hydration effect from the addition of chloride. On the other hand, the formation of ettringite and CH during corrosion was mainly studied. It can be found that they are mainly distributed from 55 to 65 degree, and are magnified in Fig. 7.

From Figs. 7(a) and 7(b) for samples immersed in the water, the intensity of CH also increased with the immersion time due to the formation of CaOH from continuous hydration reaction, while the AFt phase was usually neglected for the concretes in the water. With concretes immersed into the 10% Na_2SO_4 solution B, as shown in Figs. 7(c) and 7(d), it can be clearly seen that the

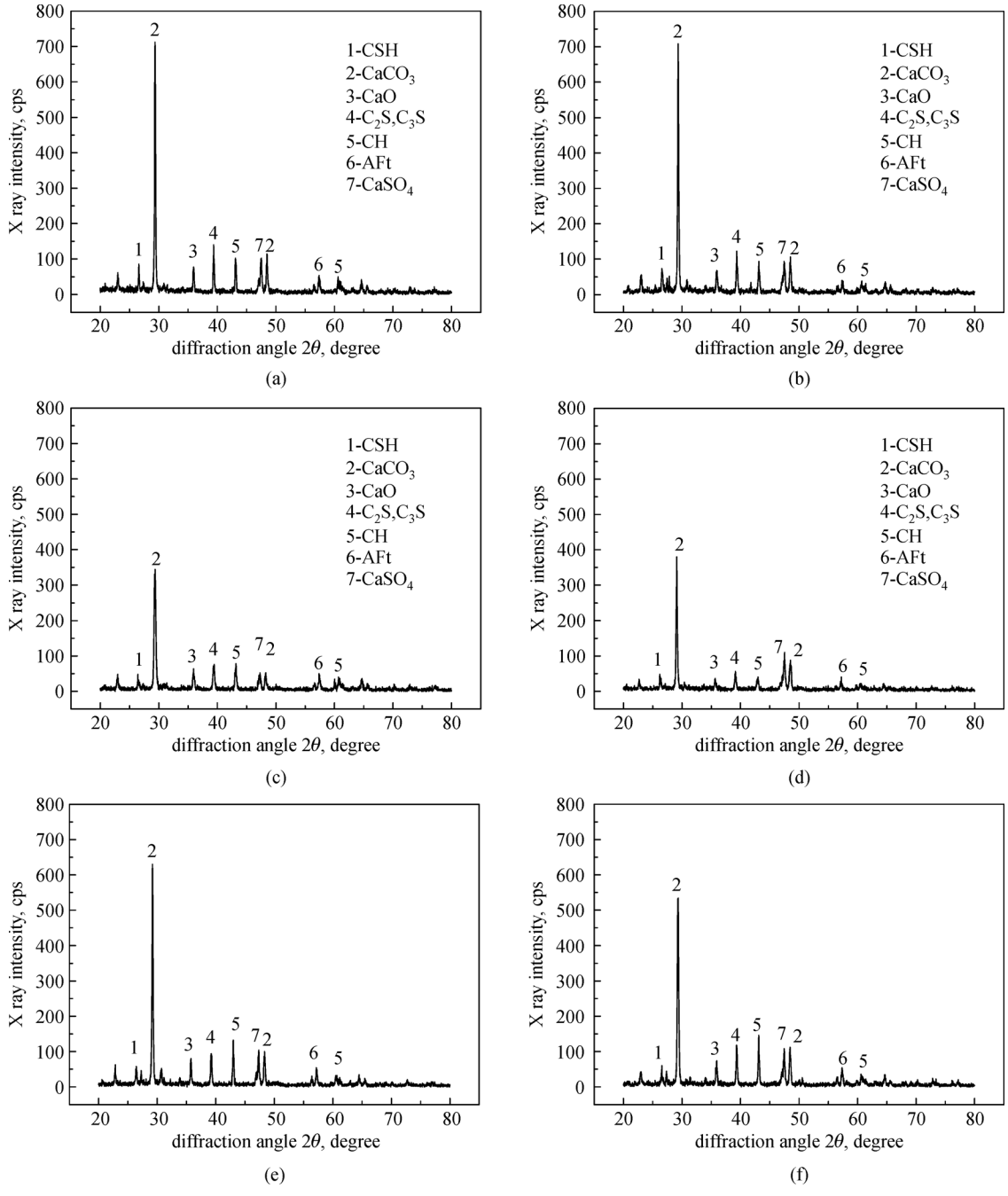

Fig. 6 XRD spectrums of the paste in different corrosion solutions at different corrosion ages. (a) water for 60 days; (b) water for 120 days; (c) 10% Na_2SO_4 for 60 days; (d) 10% Na_2SO_4 for 120 days; (e) 10% NaCl-10% Na_2SO_4 for 60 days; (f) 10% NaCl-10% Na_2SO_4 for 120 days

intensity and integrated area of AFt and CH phases decreased with the increasing on immersion time, which illurstrated that the formation of CH and AFt decreased during the corrosive attack. On the other hand, compared the results in Figs. 6(c) with 6(d), the amount of $CaSO_4$ in concretes increased with the immersion time in the sulfate solution. According to the therory on concentration product, when the concentration of SO_4^{2-} and Ca^{2+} was larger than that of $CaSO_4$, the gypsum phase was precipated. Therefore, with the concretes immersed into a higher content sulfate solution, both the formation of AFt and the precipation of gypsum phase were occurred in the concretes. On the other hand, because the reaction consumed CH, the hydration reaction product $3CaO \cdot Al_2O_3 \cdot 6H_2O$ was decomposed, which finally deteriorated the compression strength of concrete. However, for the samples immersed in the composite solution with 10% NaCl and 10% Na_2SO_4, the intensity and integrated area

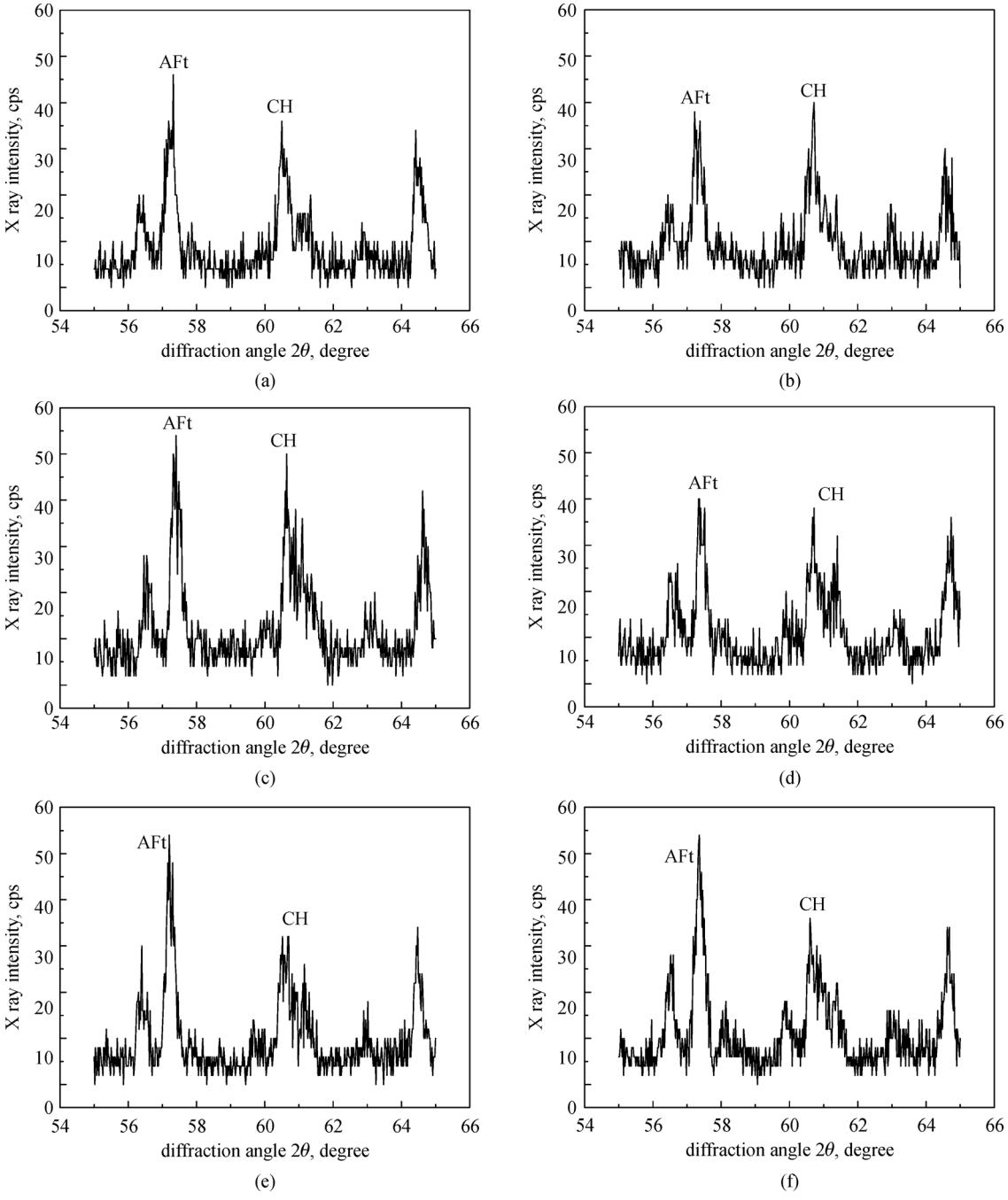

Fig. 7 X-ray diffraction chart within the scope of AFt and CH diffraction characteristic peak. (a) water for 60 days; (b) water for 120 days; (c) 10% Na_2SO_4 for 60 days; (d) 10% Na_2SO_4 for 120 days; (e) 10% NaCl-10% Na_2SO_4 for 60 days; (f) 10% NaCl-10% Na_2SO_4 for 120 days

for AFt phase in Figs. 7(e) and 7(f) was similar as those in the water, which suggested there was no obvious change on the amounts of AFt in concretes. Therefore, the corrosion on the concretes in the combined sulfate and chloride solution was limited in a shorter time. Compared the phases in Figs. 7(c)–7(e), the AFt phase in Fig. 7(d) was decomposed into the bigger gypsum phase, while the AFt phase in Fig. 7(f) kept unchange, which illusrated the existence of chloride depressed the transformation from ettringite to gypsum phase. The XRD results were consistent with the results from ultrasonic detection.

3.5 Microstructure on corrosion products

Fig. 8 shows the SEM microstructure on the cement pastes from the concrete specimens immersed into B solution (10% Na_2SO_4 solution, Fig. 8(a) and 8(b)), C solution (5% NaCl + 10% Na_2SO_4 composite solution, Fig. 8(c) and

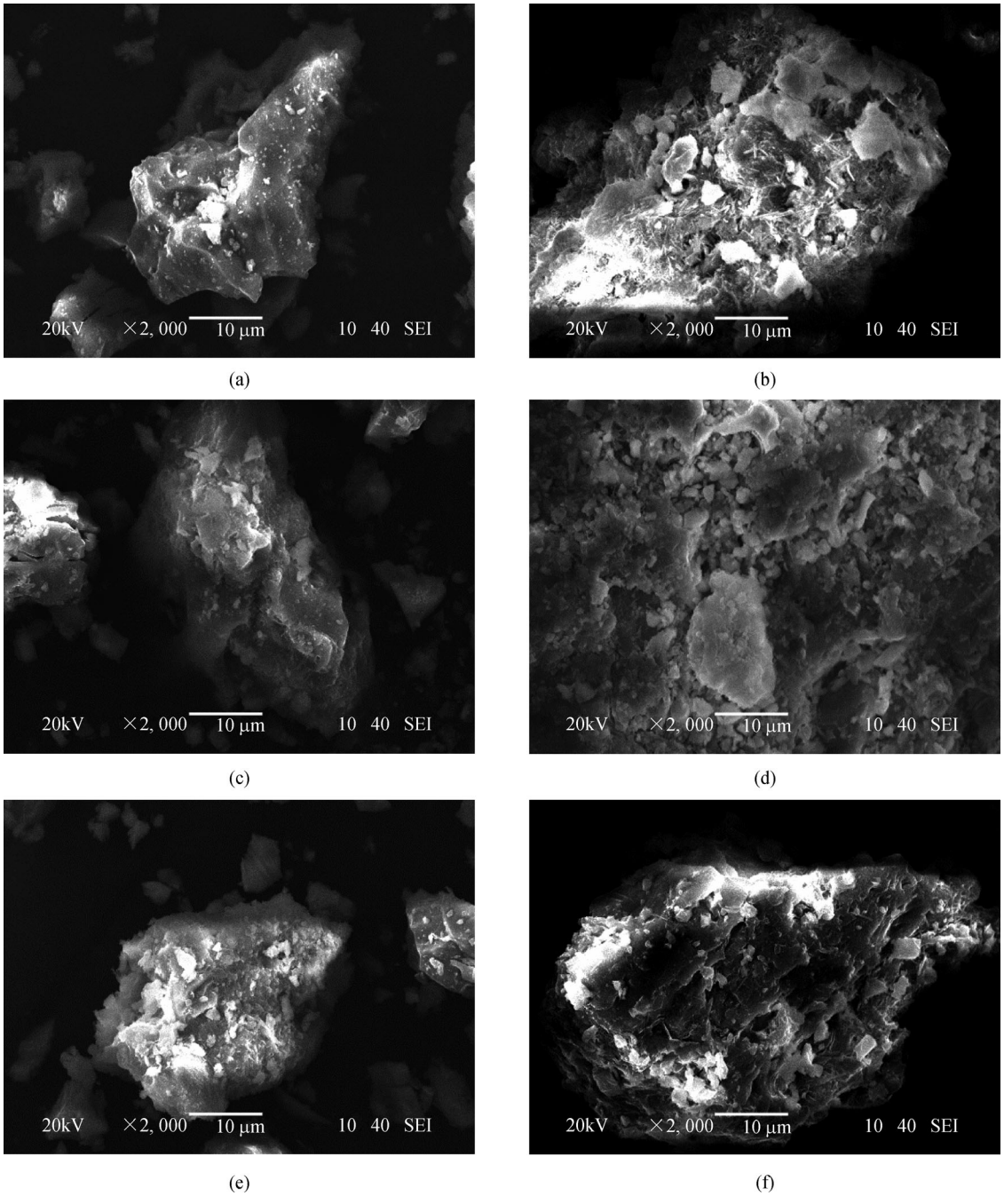

Fig. 8 SEM microstructure on corrosion products from the concretes immersed in different solution with different days. (a) water for 60 days; (b) water for 120 days; (c) 10% Na_2SO_4 for 60 days; (d) 10% Na_2SO_4 for 120 days; (e) 10% NaCl-10% Na_2SO_4 for 60 days; (f) 10% NaCl-10% Na_2SO_4 for 120 days

8(d)) and D solution (10% NaCl + 10% Na_2SO_4 composite solution, Fig. 8(e) and 8(f)) for 60 days and 210 days, respectively.

During the early stage with 60 days, the concrete was mainly composed of C-S-H gel, and no corrosion was occurred from the observation on Figs. 8(a), 8(c) and 8(e). After 210 days, large amounts of the needle ettringite and aggregated fiber gypsum phase were produced at the surface of concrete due the corrosion from sulfate in the 10% Na_2SO_4 corrosive solution, as shown in Fig. 8b. However, with the addition of chloride into sulfate solution, small amounts of corrosion products was produced in 5% NaCl + 10% Na_2SO_4 composite solution, but was completely depressed in 10% NaCl + 10% Na_2SO_4 composite solution, as shown in Fig. 8(f). Therefore, the microstructure also confirmed that the addition of chloride was beneficial to depress the formation of corrosion products, and the depressing effect also

increased with the content of chloride in the composite solution.

4 Conclusions

(1) The existence of chloride obviously decreased the corrosion of lining concrete under sulfate attack. The corrosion in the concrete was mainly occurred in the damage on the ettringite phase. The depressing effect from chloride increased with the content of chloride in the chloride-sulfate composite solution.

(2) The effect of chloride-sulfate composite solution on the damage of corrosive concretes contained three stages: initial slower enhancement on the strength, stabilization period and linear degradation period, which was independent of the composition of corrosive solution. The addition of chloride into sulfate solution mainly affected the final degradation stage through depressing the corrosion thickness.

(3) For concretes immersed in the sulfate solution, ettringite was firstly produced and then transformed into gypsum phase. Therefore the damage in concretes under sulfate solution was ettringite-gypsum mixed mode.

(4) The depressing effect from chloride addition into sulfate solution was confirmed by compression strength, XRD analysis, ultrasonic results and SEM microstructure.

Acknowledgements The authors would like to acknowledge two financial supports provided by National Science Foundation under Grant No: 51408268 and Jiangsu Natural Science Foundation under Grant No: BK20141294.

References

1. Livio L, Gabriele D M, Corrado Z. Reliabilitation of highway tunnels-techniques and procedures.In: Proceedings of AITES-ITA 2001 world tunnel congress.Vol.2, session 2–3, Bologna, 2001
2. Richards J A. Inspection maintenance and repair of tunnels: International lessons and practice. Tunnelling and Underground Space Technology, 1998, 13(4): 369–375
3. Romer M, Holzer L, Pfiffner M. Swiss tunnel structures: concrete damage by formation of thaumasite. Cement and Concrete Composites, 2003, 25(8): 1111–1117
4. Šuput J S, Mladenovic A, Cernilogar L, Olenšek V. Deterioration of mortar caused by the formation of thaumasite on the limestone cladding of some Slovenian railway tunnels. Cement and Concrete Composites, 2003, 25(8): 1141–1145
5. Leemann A, Thalmann C, Studer W. Alkali-aggregate reaction in Swiss tunnels. Materials and Structures, 2005, 38(277): 381–386
6. Inokuma A, Inano S. Road tunnel in Japan: deterioration and countermeasures. Tunnelling and Underground Space Technology, 1996, 11(3): 305–309
7. Kazuaki K, Minoru K, Tsutomu T. Structure and construction examples of tunnel reinforcement method using thin steel panels. Nippon Steel Technical Report, 2005, 92: 45–50
8. Liang Yongning,Yuan Yingshu. Mechanism of concrete destruction under sodium sulfate and magnesium sulfate solution. Journal of the chinese ceramic society, 2007, 35(4): 504–508
9. Jin Zuquan,ZhaoTiejun,Sun Wei. Study on damage to concrete attacked by sulfates. Industrial construction, 2008, 38(2): 90–93
10. Kang Yong,Li Xiaohong,Xu Mou,Yang Guang, Xia Xiaoquan. Application of water quality analysis in Beacon Hill tunnel corrosion protection design in Chongqing. The chinese journal of geological hazard and control,2005, 16(2): 80–83
11. Chen J, Jiang M, Zhu J. Damage evolution in cement mortar due to erosion of sulfate. Corrosion Science, 2008, 50(9): 2478–2483
12. Chu H, Chen J. Evolution of viscosity of concrete under sulfate attack. Construction & Building Materials, 2013, 39: 46–50
13. Brown P W, Badger S. The distributions of bound sulfates and chlorides in concrete subjected to mixed NaCl,$MgSO_4$,Na_2SO_4, attack. Cement and Concrete Research, 2000, 30(10): 1535–1542
14. Al-Amoudi O S B, Maslehuddin M, Abdul-Al Y A B. Role of chloride ions on expansion and strength reduction in plain and blended cements in sulfate environments. Construction & Building Materials, 1995, 9(1): 25–33
15. Tumidajski P J, Chan G W. Effect of sulfate and carbon dioxide on chloride diffusivity. Cement and Concrete Research, 1996, 26(4): 551–556
16. Jin Zuquan,Sun Wei,Zhang Yunsheng,Lai Jianzhong. Effect of chloride on damage of concrete attacked by sulfate. Journal of wuhan university of technology, 2006, 28(3): 42–46
17. Reju R, Jacob G J. Investigations on the chemical durability properties of Ultra High Performance Fibre Reinforced Concrete. International Conference on Green Technologies, 2012,181–185
18. Al-Amoudi O, Rasheeduzzafar A A, Maslehuddin M. Influence of Sulfate Ions on Chloride-Induced Reinforcement Corrosion in Portland and Blended Cement Concretes. Cement, Concrete and Aggregates, 1994, 16(16): 3–11
19. Chiker T, Aggoun S, Houari H, Siddique R. R. Sodium sulfate and alternative combined sulfate/chloride action on ordinary and self-consolidating PLC-based concretes. Construction & Building Materials, 2016, 106(1): 342–348
20. Pradhan B. Corrosion behavior of steel reinforcement in concrete exposed to composite chloride–sulfate environment. Construction & Building Materials, 2014, 72: 398–410
21. Cong C, Yang L. Experimental research on concrete permeability of underground structure. Rock and Soil Mechanics, 2011, 32(8): 2379–2385
22. Pan Hongke, Niu Jishou, Yang Linde, Tang Yongjing. The durability deterioration model based on carbonation for underground concrete structures. Engineering mechanics, 2008, 25(7): 172–178
23. Lei Mingfeng, Peng Limin, Shi Chenghua. Experimental study on evolution law of mechanical properties of tunnel structure suffering ambient sulfate. China civil engineering journal, 2013, 46(1): 126–132
24. Zhang Fengjie, Yuan Yingshu, Du Jianmin.Ultrasonic detection in concrete structures of damage from sulfate attack. Journal of China University of Mining & Technology, 2011, 40(3): 373–378

25. Du Jianmin J R, Ji Y. The reduction in sulfate corrosion of concrete by chloride ion. Journal of China University of Mining & Technology, 2012, 41(6): 906–911
26. Luo L. Approximate formula of integral intensity in X optical diffraction. College Physics, 2004, 23(12): 49–50
27. Zhang Q, Liu GL, Cheng CH, Du HX. Experimental study on high strength concrete after high temperature based on XRD. China concrete and cement products, 2015, 3: 9–11